

The metabolic cost of neural information

Simon B. Laughlin¹, Rob R. de Ruyter van Steveninck² and John C. Anderson^{1,3}

¹ Department of Zoology, University of Cambridge, Cambridge CB2 3EJ, UK

² NEC Research Institute, 4 Independence Way, Princeton, New Jersey 08540, USA

³ Sussex Centre for Neuroscience, University of Sussex, Brighton BN1 9QG, UK

Correspondence should be addressed to S.B.L. (SL104@cam.ac.uk)

We derive experimentally based estimates of the energy used by neural mechanisms to code known quantities of information. Biophysical measurements from cells in the blowfly retina yield estimates of the ATP required to generate graded (analog) electrical signals that transmit known amounts of information. Energy consumption is several orders of magnitude greater than the thermodynamic minimum. It costs 10^4 ATP molecules to transmit a bit at a chemical synapse, and $10^6 - 10^7$ ATP for graded signals in an interneuron or a photoreceptor, or for spike coding. Therefore, in noise-limited signaling systems, a weak pathway of low capacity transmits information more economically, which promotes the distribution of information among multiple pathways.

Neural processing is metabolically expensive. The human brain accounts for 20% of resting oxygen consumption, and half of this energy drives the pumps that exchange sodium and potassium ions across cell membranes¹. Because these pumps are maintaining the ionic concentration gradients that power electrical signaling by neurons, 10% of a resting human's energy is used to keep the brain's batteries charged. In the rabbit retina, second messenger systems, synapses and ion pumps make large contributions to a high metabolic rate^{2,3}. Therefore, when the basic cellular mechanisms for signaling and information processing are concentrated in brains and sense organs, the metabolic demands are considerable.

These metabolic demands could be large enough to influence the design, function and evolution of brains and behavior. Comparative studies suggest that the metabolic expense of maintaining the brain throughout life⁴, or the demands made by the developing brain on the maternal energy budget⁵, have limited the sizes of primate brains. The human brain's susceptibility to anoxia and its precise local regulation of cerebral blood flow also suggest that the supply of energy limits neural function. If metabolic energy is limiting, then neurons, neural codes and neural circuits will have evolved to reduce metabolic demands. Two elegant theoretical analyses show that metabolic efficiency can profoundly influence neural coding. The minimization of metabolic cost promotes the distribution of signals over a population of weakly active cells^{6,7}.

Although metabolic energy is clearly important in determining neural function, we lack basic data on the quantitative relationships between energy and information in nervous systems. Precisely how much energy must a neuron consume to do a given amount of useful work, transmitting and processing information? How does energy consumption scale with the quantity of information that neurons handle? We can now address these fundamental questions because we have recently measured the quantities of information transmitted by photoreceptors and interneurons of the intact blowfly retina⁸ and can use biophysical

data to estimate the amount of energy required to transmit these signals. We find that information is expensive, and that, for a given communication channel, the cost per bit increases with bit rate. Thus metabolic cost can have a profound influence on the structure, function and evolution of cell signaling systems, neurons, neural circuits and neural codes.

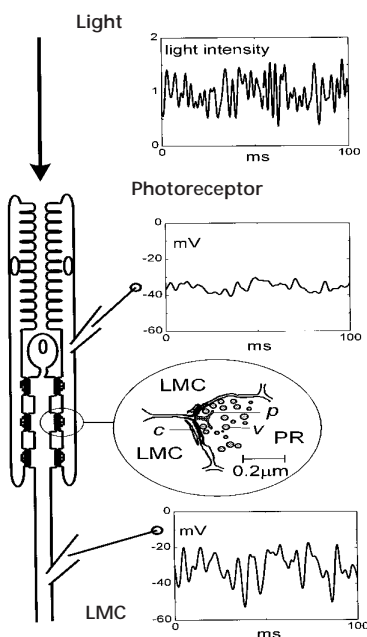
Results

THE METABOLIC COST OF INFORMATION IN A PHOTORECEPTOR Information transmission rate, measured in bits per second, is a useful measure of the neural work done by photoreceptors and interneurons of the fly compound eye, for the following reasons. Increasing the number of bits transmitted per cell improves the retinal image by increasing the number of gray levels coded per second per pixel. A number of studies conclusively demonstrate that the large monopolar cell (LMC), the second-order retinal neuron, is optimized to maximize bit rate⁹. We have recently measured the rates at which retinal cells transmit information under daylight conditions⁸. Cells were driven by randomly modulating the light intensity of an LED (Fig. 1), with a depth of modulation (contrast) that resembled natural signals. Photoreceptors responded to this random test stimulus with a graded modulation in membrane potential that encoded the fluctuations in light level (Fig. 1). The photoreceptor signal is contaminated by noise, both signal and noise have a Gaussian distribution, and the system is approximately linear over this natural contrast range. Under these conditions, we can determine the rate at which the photoreceptor transmits information, I , from measurements of the power spectra of signal, $S(f)$ and noise, $N(f)$, by applying Shannon's equation

$$I = \int_0^{\infty} df \cdot \log_2 \left[1 + \frac{S(f)}{N(f)} \right] \quad (1)$$

We estimated $I = 1000$ bits per second for the fully light-adapted cell, but we expect lower rates under natural conditions

Fig. 1. Cells, synapses and signals in blowfly compound eye. Photoreceptors and an LMC of the blowfly retina code light level in a single pixel of the compound eye. Six photoreceptors carrying the same signal converge on a single LMC and drive it via multiple parallel synapses. For clarity, only two of the six photoreceptors are depicted. The signals are intracellular recordings of the graded changes of membrane potential induced by a randomly modulated light source. Analysis of these analog responses yielded the rate at which photoreceptors and LMCs transmit information⁸. The oval inset shows a photoreceptor-to-LMC synapse. The presynaptic site on the photoreceptor axon terminal (PR), contains synaptic vesicles (*v*), grouped around a prominent presynaptic ribbon (*p*). This release site faces four postsynaptic elements, containing cisternae (*c*). The central pair of elements are invariably the dendrites of the two parallel LMCs, as captured in this tracing of an electron microscope section⁴³.



second-messenger cascade passes the signal from rhodopsin to ion channel, amplifies the signal, and consumes energy in at least two processes, the phosphorylation of intermediates and the transfer of a second messenger, calcium ions, between compartments¹⁵. However, the costs of the cascade, although appreciable, are unlikely to inflate consumption by an order of magnitude for the following reason. We find that a photoreceptor transducing 10^6 photons per second consumes $7 \cdot 10^9$ ATP molecules per second. Consequently the cascade would have to hydrolyze almost 10^4 ATP molecules per transduced photon to equal the energy demands of the electrical current. We conclude that our estimate of $7 \cdot 10^6$ ATP molecules per bit is a conservative figure that is strongly supported by independent experimental data.

Our costing of phototransduction suggests an important principle that can simplify the calculation of neural energy budgets. Neural signaling and processing can involve a cascade of amplification in which increasing numbers of molecules are recruited at each

because natural signals contain correlations that are not present in our random stimuli.

We can now estimate the cost of a bit of information by determining the metabolic energy required to code information under these fully light-adapted conditions. We recorded from five photoreceptors that were stimulated at the same daylight level, 10^6 effective photons per receptor per second. These photoreceptors had an average membrane potential, E_m , of -33 ± 6 mV. Injection of current yielded an average input resistance of 7.1 ± 1.8 M Ω , giving a mean total conductance for the single photoreceptor, g_{total} of 141 nS. We incorporate these electrical data into a simple electrical model of the photoreceptor membrane (Fig. 2), based on published biophysical data. The model calculates the ionic currents that flow across the membrane during signaling. These ion fluxes define the rate at which a vigorous Na/K exchange pump^{10–12} must hydrolyze ATP to maintain the ionic concentration gradients that are driving currents across the membrane. Dividing this rate of ATP consumption, $7.5 \cdot 10^9$ ATP molecules per second, by the information transmission rate, 1000 bits per second, gives the metabolic cost for sensory information, $7 \cdot 10^6$ ATP molecules per bit.

Measurements of the oxygen consumed by isolated insect retinas confirm that our estimate of ATP consumption, and hence bit cost, is of the right order of magnitude. In the drone bee retina¹³ each photoreceptor consumes $2 \cdot 10^9$ ATP molecules per second, compared with our estimate in the blowfly of $7 \cdot 10^9$ ATP molecules per second. In the blowfly there are approximately 35,000 photoreceptors per retina¹⁴. Consequently, aerobic glycolysis must consume $6.5 \cdot 10^{-5}$ mls O_2 per minute to meet our estimated consumption of ATP. The measured value is almost identical, $6 \cdot 10^{-5}$ mls O_2 per minute¹¹.

Our value, $7 \cdot 10^6$ ATP molecules per bit, is a lower bound because photoreceptors will transmit information at lower rates under natural conditions. Moreover, by basing our cost on electrical current, we exclude the intermediate steps in phototransduction. A

successive step. The last stage, which often results in the flow of ionic current across the cell membrane (synaptic transmission), will consume the most energy. This could be why ion pumps are responsible for over half of the human brain's energy consumption³. When ion currents dominate energy requirements, then reasonable lower bounds for metabolic costs can be calculated from conductance measurements, as demonstrated here, without recourse to direct measurements of oxygen consumption. We will use this principle again when we consider the chemical synapse.

THE COST OF INFORMATION IN A RETINAL NEURON

Six photoreceptors carrying the same signal converge on a second order neuron, the LMC. Each photoreceptor drives the

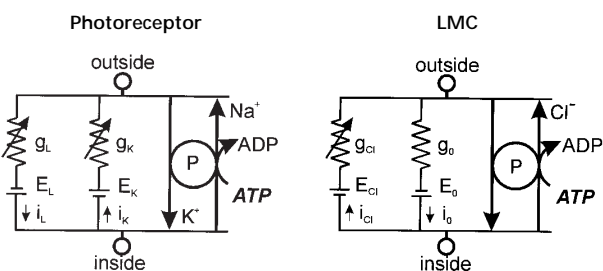


Fig. 2. The electrical models of photoreceptor and LMC membranes. By estimating the currents required to generate electrical signals, the models calculate the rates at which pumps (P) must hydrolyze ATP to sustain electrical signalling. Symbols, Photoreceptor: g_L , light-gated conductance; i_L , light gated current; g_K , voltage-gated potassium conductance; i_K , potassium current; P, Na/K exchange pump. LMC: g_{Cl} , histamine-gated chloride conductance; i_{Cl} , histamine-gated chloride current; g_o , non-specific cation conductance assumed to oppose chloride conductance; i_o , non-specific cation current; P, chloride pump (see Methods).

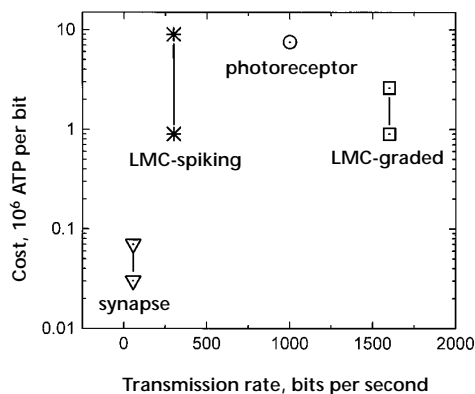


Fig. 3. The cost of a bit of information plotted against information transmission rate for a single chemical synapse, a hypothetical LMC using spikes, and the graded signals of a photoreceptor and an LMC. The ranges cover assumptions made in calculating costs. For the transmission rate of the hypothetical spiking LMC, we use the highest value yet measured in a sensory neuron²³.

LMC, with 220 identical parallel synapses, giving 1320 synapses in all (Fig. 1)¹⁶. At each synapse a fast neurotransmitter, histamine, gates chloride channels¹⁷ to generate a graded response in the LMC. This analog signal is an inverted, amplified and high-pass-filtered version of the photoreceptor input (Fig. 1). Using the random stimuli applied to photoreceptors, we found that, as a result of convergence, the LMC is more reliable than a single photoreceptor, and transmits information at a higher rate, 1600 bits per second⁸.

Again, a simple electrical model (Fig. 2) calculates the currents that flow during the LMC response, and hence the ATP consumption by pumps. In the model, the postsynaptic chloride current is generated by the histamine-gated chloride conductance g_{Cl} , with a reversal potential E_{Cl} of -65 mV¹⁸. The counter-current that holds the LMC membrane potential above E_{Cl} has not been identified. We assume a nonspecific cation conductance, g_0 , with a reversal potential E_0 of 0 mV. If one assumes that the chloride pump is not electrogenic, then the simple circuit model for the postsynaptic LMC membrane (Fig. 2) is equivalent to equations 2,3,5 and 6 in the receptor model (Methods). Inserting published measurements of total membrane conductance and membrane potential^{18,19}, the LMC model gives a postsynaptic chloride current in bright light of 0.66 nA. A chloride pump maintains E_{Cl} ²⁰, but it has not been characterized. Known pumps transfer between 1 and 3 chloride ions per ATP hydrolyzed. Equating the synaptic influx of chloride ions with pump efflux gives a threefold range of pump consumption, $1.4 \cdot 10^9$ to $4.1 \cdot 10^9$ ATP molecules per LMC per second. Dividing by the measured bit rate gives a range of metabolic costs for information, $9 \cdot 10^5$ to $3 \cdot 10^6$ ATP molecules per bit.

Note that the LMC codes at a lower cost per bit than the photoreceptor. Although several assumptions had to be made to calculate ion fluxes and pump rates in LMCs, this conclusion is likely to be correct. The LMC has a lower membrane conductance¹⁸ and, through redundancy reduction and signal convergence⁹, transmits information at a higher rate⁸. In addition, photoreceptors employ a large membrane area to capture and transduce photons, and this increases their overall conductance.

THE COST OF INFORMATION AT A CHEMICAL SYNAPSE

Each of the 1320 photoreceptor synapses driving an LMC is a tetrad with an average contact area $200 \text{ nm} \times 500 \text{ nm}$ and a prominent presynaptic bar (Fig. 1). From the number of identical synapses¹⁶ and the information rates in a photoreceptor and an LMC, we have previously calculated that each synapse transmits 55 bits per second⁸. Because identical synapses contribute equally to the total LMC chloride conductance, g_{Cl} , the post-synaptic chloride current at one synapse accounts for $1/1320$ of the LMC ATP consumption, calculated above. Dividing consumption by transmission rate gives a range of metabolic costs for information at a single chemical synapse of $2 \cdot 10^4$ to $6 \cdot 10^4$ ATP molecules per bit.

This estimate of synaptic cost is based on postsynaptic current and ignores all presynaptic mechanisms. On present evidence, this simplification will not significantly change our conclusions. Using experimental data, we estimate that the costs of neurotransmitter uptake and vesicle refilling total less than 10% of the postsynaptic current (see Methods). Estimates of presynaptic calcium flux vary from 200 to $1.3 \cdot 10^4$ ions per vesicle discharged²¹. With 240 vesicles released per second (see Methods), and 1 calcium ion pumped per ATP²², presynaptic calcium fluxes would add from 2% to 60% to our synaptic costs. The energy used to recycle vesicles is unknown but, given a vesicle discharge rate of 240 per second, it would need to be $3 \cdot 10^3$ ATPs per vesicle to equal the postsynaptic cost. We conclude that our lower bound for synaptic cost is of the right order of magnitude and, on the present evidence, within a factor of two of the real cost.

BIT RATE VERSUS COST IN NOISE-LIMITED SYSTEMS

The low capacity (55 bits per second) synapse transmits at a much lower cost per bit than the high capacity (1600 bits per second) interneuron, the LMC (Fig. 3). Thus, as in many communication systems, a lower transmission rate is cheaper. This trade-off between cost and capacity is enforced by the stochastic nature of cell signaling. Cost is proportional to N , the number of elementary stochastic events that produce signals, such as photon absorptions, channel openings, synaptic vesicle releases,

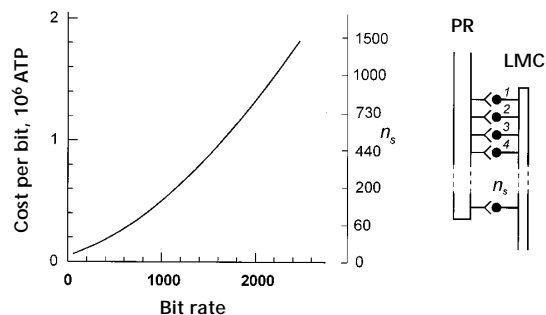


Fig. 4. The rise in cost per bit with bit rate is illustrated by modeling the transfer of signals from a photoreceptor (PR) to an LMC via a parallel array of n_s identical synapses. Each synapse carries an identical signal that is contaminated by noise. The bit rate for transmission from photoreceptor to LMC is increased by using more synapses to improve the overall signal-to-noise ratio (see Methods). The number of synapses involved, n_s , is indicated on the scale to the right of the graph. The values of rate and cost are based on estimates of signal and noise power spectra at a single synapse⁸ and on estimates of the cost of synaptic transmission derived in this paper.

receptor or G-protein activation. The signal-to-noise power ratio also increases as N , and information as $\log_2(N)$ (see Methods), to produce a savage law of diminishing returns. We illustrate this relationship (Fig. 4) by modeling the array of parallel synapses that connects a photoreceptor to an LMC (see Methods). To increase the rate at which information is transmitted between this pair of cells, the number of synapses must be increased (see Methods, eqn. 7), and this increases the cost of transmitting a bit (Fig. 4). It would be more economical to transmit the extra information through a second pair of cells. Thus, in the face of fundamental noise limitations, energy efficiency promotes the division of information among parallel pathways, each of low capacity, so favoring the use of parallel messenger systems within cells, and sparse coding in neural networks⁶. A similar conclusion has been reached independently by extrapolating from an energy-efficient electronic cochlea to neural mechanisms⁷.

THE COST OF TRANSMITTING INFORMATION BY SPIKES

The photoreceptors and interneurons of the fly retina use graded (analog) responses because they carry information at high rates. Perhaps spike coding is more economical. We investigated this possibility by estimating the cost for spike transmission down an LMC and comparing it to our estimate of the analog cost (derived above). The LMC's graded synaptic signal is conducted along its axon to output synapses, approximately 425 μm away. Transmission is passive¹⁹; consequently its cost is included in generation of postsynaptic LMC response and therefore is $9 \cdot 10^5$ to $3 \cdot 10^6$ ATP molecules per bit. Were a spike to carry information over this same distance, it would transiently depolarize the entire length of the axon by 100 mV. The known axon capacitance¹⁹ defines the minimum sodium ion influx needed to propagate the spike and hence a pump consumption of $9 \cdot 10^6$ ATP molecules per spike. A sensory spike carries between 1 and 10 bits of information²³, giving a range of costs, $9 \cdot 10^5$ to $9 \cdot 10^6$ ATP molecules per bit. This cost per bit brackets the analog costs (Fig. 3), leading us to conclude that action potentials do not greatly enhance metabolic efficiency over short distances, at least in this unmyelinated insect axon. A primary function of spikes could be to reduce the effects of synaptic noise⁷ by tightly coupling vesicle release to presynaptic action potentials.

Discussion

IS INFORMATION COSTLY?

Metabolic efficiency will only be an important determinant of the evolution and design of signaling systems when metabolic costs impose a significant penalty on the parent organism. Our estimate of photoreceptor ATP consumption in bright light is equivalent to 8% of the total consumption by the resting fly²⁴ and, if we add to this the consumption by LMCs, this figure approaches 10%. This consumption compares with a figure for the human brain of 20%, which is widely considered to be significant^{1,3} and could have shaped its evolution²⁵. The significance of retinal ATP consumption is reinforced by comparative studies. Blowfly photoreceptors consume more energy, gram for gram, than active mammalian muscle, metabolic investment in vision varies widely between insect species, in accordance with lifestyle and habitat (Laughlin and D.C. O'Carroll, unpublished results), and the visual systems of burrowing and cave-dwelling species are greatly reduced²⁶.

WHY IS NEURAL INFORMATION COSTLY?

Synapses and cells are using 10^5 to 10^8 times more energy than the thermodynamic minimum. Thermal noise sets a lower

limit of $k \cdot T$ Joules for observing a bit of information (k , Boltzmann's constant; T , absolute temperature, 290°K)^{27,28} and the hydrolysis of one ATP molecule to ADP releases about $25 kT$ ²⁹. It is beyond the scope of this paper to analyze the factors that increase the cost of information by five to eight orders of magnitude relative to the thermodynamic minimum, but elementary observations are instructive. At the heart of most cell signaling systems are protein molecules that code information by changing conformation. We can regard such a signaling molecule as a switch that codes a binary digit, a single bit, by flipping from one conformation to another. How fast can this molecule switch, and how much energy is needed? The motor protein kinesin cycles conformation approximately 100 times per second, hydrolyzing 1 ATP per cycle^{30,31} and does considerable mechanical work. Freed from heavy mechanical work, ion channels change conformation in roughly 100 μs ³². In principle, therefore, a single protein molecule, switching at the rate of an ion channel with the stoichiometry of kinesin, could code at least 10^3 bit per second at a cost of 1 ATP per bit. We find that a molecular system, the chemical synapse, transmits at only 5% of the rate of the single molecule but at 10^4 times the cost per bit. Highly specialized cells, the photoreceptor and the LMC interneuron, achieve the same bit rate as the molecular switch, but at 10^6 times the cost per bit. These elementary comparisons suggest that costs soar when molecules are organized into cellular systems. At least two biophysical constraints will contribute to these systems' costs. First, there is the uncertainty associated with molecular interactions. The stochastic nature of receptor activation (photon absorption), of molecular collision, of diffusion, and of vesicle release, degrades information by introducing noise (eqns. 1 and 7), thereby substantially increasing costs. Secondly, energy is required to distribute signals over relatively large distances. We suggest, therefore, that the high metabolic cost of information in systems is dictated by basic molecular and cellular constraints to cell signaling, as independently proposed by Sarpeshkar⁷ (see also Sarpeshkar, R; Ph.D. dissertation, California Institute of Technology, 1997). Because these systems' costs are substantial, further investigation of the metabolic efficiency of cell signaling has the potential to provide insights into the function, design and evolution of molecular signaling complexes, second messenger systems³³, sensory receptors, neurons, neural networks and neural codes.

Methods

MEASURING PHOTORECEPTOR MEMBRANE POTENTIAL AND CONDUCTANCE. Established techniques^{8,34,35} were used to record intracellular responses from photoreceptors R1-6 in the intact retina of the blowfly (*Calliphora vicina*) to calibrate the effective intensity of illumination of each cell by counting quantum bumps and to measure membrane resistance by injecting randomly modulated current via a single electrode-switched clamp.

CALCULATING PHOTORECEPTOR ATP CONSUMPTION Our circuit model of the photoreceptor membrane (Fig. 2) is based on biophysical measurements^{34,36}. The light-gated conductance, g_L , admits a current, i_L , with a reversal potential, $E_L = 5$ mV, given by

$$i_L = (E_m - E_L) \cdot g_L \quad (2)$$

A voltage-gated, delayed-rectifier conductance, g_K , provides a counterbalancing current of potassium ions, i_K , reversal potential $E_K = -85$ mV, given by

$$i_K = (E_m - E_K) \cdot g_K \quad (3)$$

The vigorous electrogenic pump¹⁰⁻¹² extrudes three sodium ions and

takes up two potassium ions for every ATP molecule hydrolyzed. The pump maintains the internal potassium concentration by accumulating potassium ions at a rate equal to the outward potassium current, i_K , and this specifies a net pump current,

$$i_p = \frac{i_K}{2} \quad (4)$$

Equating all currents across the model membrane

$$i_K + i_L + i_p = 0 \quad (5)$$

and specifying that total membrane conductance

$$g_{total} = g_K + g_L \quad (6)$$

gives five equations (2-6) that specify the flow of ions in this circuit. Inserting our measurements of E_m and g_{total} and published values of E_L & E_K ^{34,36}, we solve to obtain the currents flowing across the membrane of a single photoreceptor in daylight:

$$i_L = 3.6 \text{ nA}$$

$$i_K = 2.4 \text{ nA}$$

Note that the ratio between currents, $i_L:i_K$, equals the $\text{Na}^+:\text{K}^+$ ratio in the pump, and the system maintains both sodium and potassium concentrations. Inserting the value for i_K in equation 4 gives the pump current, and hence the rate of ATP hydrolysis in a single photoreceptor as $7.5 \cdot 10^9$ ATP molecules per second.

THE PRESYNAPTIC COSTS OF NEUROTRANSMITTER RELEASE AND UPTAKE. Transmitter circulates by being released from vesicles into the synaptic cleft, taken up from the cleft into the presynaptic terminal, and then pumped back into vesicles. The costs of release (presynaptic calcium fluxes, vesicle docking and release) are likely to be comparatively small because a large number of transmitter molecules are released with each vesicle. Work on the output synapses of barnacle photoreceptors³⁷ suggests that histamine is removed from the cleft by a sodium-dependent monoamine transporter in the presynaptic terminal that cotransports three sodium ions per amine molecule³⁸. Restoration of these three sodium ions by the exchange pump requires one ATP molecule. We assume that synaptic vesicles are loaded by a monoamine/proton exchange pump³⁹ that exchanges two protons, and hence hydrolyzes 0.67 ATP molecules, for every histamine translocated. Combining these two mechanisms, the rate of ATP hydrolysis is 1.67 times the circulating flux of histamine.

Three methods are used to estimate the histamine flux. The first is from the vesicle release rate. Analysis of synaptic noise⁴⁰ indicates that, at any one time, an LMC is being driven by at most 160 noise events, each with a time constant of 0.5 ms. If a noise event is a vesicle discharge, every synapse is discharging 240 vesicles per second. The average vesicle outer diameter is 35 nm and the membrane thickness 4 nm⁴¹. With a 0.1 M transmitter concentration²², each vesicle contains 600 histamine molecules. Multiplying vesicle content by release rate gives a histamine flux of $1.4 \cdot 10^5$ molecules per synapse per second. The second calculation is from the affinity of the histamine-gated chloride channels for histamine and the dimensions of the synaptic cleft. The synapses are tonically active in the midpoint of their operating range. At the very most, approximately half of the chloride channels are being gated at any one time. This requires a minimum average histamine concentration in the cleft of $40 \mu\text{M}$ ⁴². The area of synaptic contact measures 500 nm x 200 nm, and the cleft is 20 nm across, giving 50 histamine molecules per cleft. The brevity of the synaptic impulse⁴⁰ response suggests that histamine is cleared from the cleft in approximately 1 ms, giving a histamine flux of $5 \cdot 10^4$ molecules per synaptic cleft per second. The third calculation is from the histamine-gated chloride conductance, g_{Cl} , which is 13 nS from our biophysical model based on measurements of LMC input resistance. A single histamine-gated chloride channel has a conductance of 50 pS and binds three histamine molecules to open for 0.5 ms⁴². Consequently an LMC's chloride conductance binds $1.6 \cdot 10^6$ histamine molecules per second, corresponding to $1.2 \cdot 10^3$ histamine molecules per synapse per second. An LMC is one of four postsynaptic elements, and if each histamine released presynaptically is bound once by a chloride channel before being taken up, the necessary histamine

flux is $5 \cdot 10^3$ histamine molecules per synapse per second. Note that the second and third calculations ignore the losses of histamine by diffusion and by uptake from the cleft prior to channel activation.

To avoid underestimating synaptic costs, we take the highest (first) estimate of histamine flux, which gives an ATP consumption of $1.67 \times 1.4 \cdot 10^5$ or roughly $2 \cdot 10^5$ ATP molecules per synapse per second.

BIT COST VERSUS RATE FOR AN ARRAY OF PHOTORECEPTOR-TO-LMC SYNAPSES. We consider a signal carried from photoreceptor to LMC by a parallel array of identical synapses. The power density spectrum for the optimal signal, $S(f)$, and for noise, $N(f)$, at a single synapse has been estimated experimentally⁸, using a signal of rms contrast 0.316. An array of n_s synapses transmits information at a rate, I , of

$$I = \int_0^\infty df \cdot \log_2 \left[1 + \frac{n_s \cdot S(f)}{N(f)} \right] \quad \text{bits per second.} \quad (7)$$

The rate of ATP consumption by the array is n_s times the consumption by a single synapse, which we calculate from the postsynaptic chloride flux derived in the main body of the text to be $4 \cdot 10^6$ ATP molecules per second.

Acknowledgements

We would like to thank W. Bialek, D. Bray, R. Carpenter, R.C. Hardie, J.H. van Hateren and D.C. O'Carroll for their comments and suggestions, and A. Ames for his encouragement and an excellent introduction to the energetics of neural function.

RECEIVED 19 FEBRUARY; ACCEPTED 18 MARCH 1998

1. Kety, S.S. in *Metabolism of the Nervous System* (ed. Richter, D.) 221–237 (Pergamon, London, 1957).
2. Ames, A. Energy-requirements of CNS cells as related to their function and to their vulnerability to ischemia - a commentary based on studies on retina. *Can. J. Physiol. Pharmacol.* **70**, S158–S164 (1992).
3. Ames, A. in *Mitochondria and Free Radicals in Neurodegenerative Disease* (eds Beal, M.F., Howell, N. & Bodis-Wollner, I.) 17–27 (Wiley-Liss, New York, 1997).
4. Aiello, L.C. & Wheeler, P. The expensive tissue hypothesis: the brain and the digestive system in human and primate evolution. *Curr. Anthropol.* **36**, 199–221 (1995).
5. Martin, R.D. Scaling of the mammalian brain - the maternal energy hypothesis. *News In Physiol. Sci.* **11**, 149–156 (1996).
6. Levy, W.B. & Baxter, R.A. Energy-efficient neural codes. *Neural Computation* **8**, 531–543 (1996).
7. Sarpeshkar, R. Analog versus digital: extrapolating from electronics to neurobiology. *Neural Computation* (in press, 1998).
8. de Ruyter van Steveninck, R.R. & Laughlin, S.B. The rate of information-transfer at graded-potential synapses. *Nature* **379**, 642–645 (1996).
9. Laughlin, S.B. Matching coding, circuits, cells, and molecules to signals - general principles of retinal design in the fly's eye. *Prog. Ret. Eye. Res.* **13**, 165–196 (1994).
10. Gerster, U., Stavenga, D.G. & Backhaus, W. Na^+/K^+ pump activity in photoreceptors of the blowfly Calliphora: A model analysis based on membrane potential measurements. *J. Comp. Physiol. A.* **180**, 113–122 (1997).
11. Hamdorf, K., Hochstrate, P., Hoglund, G., Burbach, B. & Wiegand, U. Light activation of the sodium-pump in blowfly photoreceptors. *J. Comp. Physiol. A.* **162**, 285–300 (1988).
12. Jansonius, N.M. Properties of the sodium-pump in the blowfly photoreceptor cell. *J. Comp. Physiol. A.* **167**, 461–467 (1990).
13. Tsacopoulos, M., Veuthey, A.L., Saravelos, S.G., Perrotet, P. & Tsoupras, G. Glial-cells transform glucose to alanine, which fuels the neurons in the honeybee retina. *J. Neurosci.* **14**, 1339–1351 (1994).
14. Beersma, D.G.M., Stavenga, D.G. & Kuiper, J.W. Retinal lattice, visual field and binocularities in flies. *J. Comp. Physiol.* **119**, 207–220 (1977).
15. Hardie, R.C. & Minke, B. Phosphoinositide-mediated phototransduction in *Drosophila* photoreceptors - the role of Ca^{2+} and *trp*. *Cell Calcium* **18**, 256–274 (1995).
16. Nicol, D. & Meinertzhagen, I.A. An analysis of the number and composition of the synaptic populations formed by photoreceptors of the fly. *J. Comp. Neurol.* **207**, 29–44 (1982).
17. Hardie, R.C. A histamine-activated chloride channel involved in neurotransmission at a photoreceptor synapse. *Nature* **339**, 704–706 (1989).
18. Laughlin, S.B. & Osorio, D. Mechanisms for neural signal enhancement in the blowfly compound eye. *J. Exp. Biol.* **144**, 113–146 (1989).

19. van Hateren, J.H. & Laughlin, S.B. Membrane parameters, signal transmission, and the design of a graded potential neuron. *J. Comp. Physiol. A* **166**, 437–448 (1990).
20. Uusitalo, R.O. & Weckström, M. The regulation of chloride homeostasis in the small nonspiking visual interneurons of the fly compound eye. *J. Neurophysiol.* **71**, 1381–1389 (1994).
21. Borst, J.G.G. & Sakmann, B. Calcium influx and transmitter release in a fast CNS synapse. *Nature* **383**, 431–434 (1996).
22. Hall, Z.W. *An introduction to molecular neurobiology*, 555 (Sinauer, Sunderland, Mass., 1992).
23. Rieke, F., Warland, D., de Ruyter van Steveninck, R.D. & Bialek, W. *Spikes - exploring the neural code*, 395 (MIT Press, Cambridge, Mass., 1997).
24. Keister, M. & Buck, J. in *The Physiology of Insecta* 2nd edn Vol. 6 (ed. Rockstein, M.) (Academic Press, N.Y., 1974).
25. Aiello, L.C. Brains and guts in human evolution: The expensive tissue hypothesis. *Braz. J. Genetics* **20**, 141–148 (1997).
26. Diamond, J.M. Competition for brain space. *Nature* **382**, 756–757 (1996).
27. Szilard, L. Über die Entropieverminderung in einem thermodynamischen System bei Eingriffen intelligenter Wesen. *Z. Physik* **53**, 840–856 (1929).
28. Leff, H.S. & Rex, A.F. *Maxwell's Demon: Entropy, Information, Computing*, 349 (Adam Hilger, Bristol, 1990).
29. Howard, J. The movement of kinesin along microtubules. *Ann. Rev. Physiol.* **58**, 703–729 (1996).
30. Hua, W., Young, E.C., Fleming, M.L. & Gelles, J. Coupling of kinesin steps to ATP hydrolysis. *Nature* **388**, 390–393 (1997).
31. Schnitzer, M.J. & Block, S.M. Kinesin hydrolyses one ATP per 8-nm step. *Nature* **388**, 386–390 (1997).
32. Hille, B. *Ionic Channels of Excitable Membranes*, 607 (Sinauer, Sunderland, Mass., 1992).
33. Bray, D. Signaling complexes. *Ann. Rev. Biophys.* (in press, 1998).
34. Weckström, M., Hardie, R.C. & Laughlin, S.B. Voltage-activated potassium channels in blowfly photoreceptors and their role in light adaptation. *J. Physiol. (Lond.)* **440**, 635–657 (1991).
35. Weckström, M., Kouvalainen, E. & Juusola, M. Measurement of cell impedance in frequency-domain using discontinuous current clamp and white-noise-modulated current injection. *Pflügers Arch.-Eur. J. Physiol.* **421**, 469–472 (1992).
36. Hardie, R.C. Whole-cell recordings of the light-induced current in dissociated *Drosophila* photoreceptors - evidence for feedback by calcium permeating the light-sensitive channels. *Proc. R. Soc. Lond. B* **245**, 203–210 (1991).
37. Stuart, A.E., Morgan, J.R., Mekeel, H.E., Kempter, E. & Callaway, J.C. Selective, activity-dependent uptake of histamine into an arthropod photoreceptor. *J. Neurosci.* **16**, 3178–3188 (1996).
38. Sonders, M.S. & Amara, S.G. Channels in transporters. *Current Opinion In Neurobiology* **6**, 294–302 (1996).
39. Schuldiner, S., Shirvan, A. & Linial, M. Vesicular neurotransmitter transporters - from bacteria to humans. *Physiol. Rev.* **75**, 369–392 (1995).
40. Laughlin, S.B., Howard, J. & Blakeslee, B. Synaptic limitations to contrast coding in the retina of the blowfly *Calliphora*. *Proc. R. Soc. Lond. B* **231**, 437–467 (1987).
41. Fröhlich, A. Freeze-fracture study of an invertebrate multiple-contact synapse - the fly photoreceptor tetrad. *J. Comp. Neurol.* **241**, 311–326 (1985).
42. Skingsley, D.R., Laughlin, S.B. & Hardie, R.C. Properties of histamine-activated chloride channels in the large monopolar cells of the dipteran compound eye - a comparative-study. *J. Comp. Physiol. A* **176**, 611–623 (1995).
43. Meinertzhagen, I.A. & O'Neil, S.D. Synaptic organization of columnar elements in the lamina of the wild-type in *Drosophila melanogaster*. *J. Comp. Neurol.* **305**, 232–263 (1991).